



HAL
open science

Measurement of index modulation along Fiber Bragg Gratings by Side Scattering and Local Heating methods

Nicolas Roussel, Sylvain Magne, Christophe Martinez, Pierre Ferdinand

► **To cite this version:**

Nicolas Roussel, Sylvain Magne, Christophe Martinez, Pierre Ferdinand. Measurement of index modulation along Fiber Bragg Gratings by Side Scattering and Local Heating methods. *Optical Fiber Technology*, 1999, 5, pp.119-132. cea-01840687

HAL Id: cea-01840687

<https://cea.hal.science/cea-01840687>

Submitted on 16 Jul 2018

HAL is a multi-disciplinary open access archive for the deposit and dissemination of scientific research documents, whether they are published or not. The documents may come from teaching and research institutions in France or abroad, or from public or private research centers.

L'archive ouverte pluridisciplinaire **HAL**, est destinée au dépôt et à la diffusion de documents scientifiques de niveau recherche, publiés ou non, émanant des établissements d'enseignement et de recherche français ou étrangers, des laboratoires publics ou privés.

Measurement of Index Modulation along Fiber Bragg Gratings by Side Scattering and Local Heating Techniques

Nicolas Roussel,¹ Sylvain Magne, Christophe Martinez, and Pierre Ferdinand

LETI-CEA (Technologies Avancées), DEIN-SPE, CEA / Saclay, 91191 Gif-sur-Yvette, France

Received June 16, 1998

A method for measurement of index modulation profile along fiber Bragg gratings is described which uses a hot finger that selectively heats some fringes. Results obtained from this local heating technique and side scattering technique are reviewed and compared. © 1999 Academic Press

Key Words: fiber Bragg grating; index modulation; local heating; side scattering.

INTRODUCTION

Fiber Bragg gratings (FBGs) are increasingly used for telecommunication, instrumentation, and sensors. In some cases, as in instrumentation and smart structures technology, there is the need to know exactly where the grating is photo-written along the fiber. For instance, it is necessary to accurately localize a fiber Bragg grating prior to fixing it onto a piezoelectric stack actuator [1] or a thermal head consisting of a microheater array [2] or coating it with resistive or piezoelectric materials [3] for making spectral modulators. In the same way, to serve as a strain transducer in a precise location in a composite panel (e.g., near a hole to map stress concentration), a grating has to be accurately localized as well.

In addition, some applications require not only knowledge of where the grating is but also a measurement of its refractive index modulation. In instrumentation, for instance, there is a growing need for chirped gratings acting as dispersion compensators. Such gratings provide the reflections of different wavelength components of a broadened pulse at specific locations along their length and therefore compen-

sate for its broadening. Their spectral characteristics could be accurately tailored [4] or arbitrarily controlled in a flexible manner [1].

In a general way, the measurement of the index modulation profile provides a means to calibrate and optimize the Bragg grating photo-inscription setup, for instance, to obtain apodized gratings.

Fiber gratings are characterized by their complex coupling coefficients $K(x)$ along the grating length. At least four methods have been described to obtain a distributed measurement of this coefficient. The first method is side scattering [4]. The second method relies on interferometric measurements [5], [6]. The third method is optical coherence-domain reflectometry (OCDM) [7], [8], and the fourth method is optically induced localized phase shift (also called optical space-domain reflectometry (OSDR) [9].

The side scattering method relies on the side diffraction of a probe beam by the fiber grating and only yields the modulus of $K(x)$ (i.e., the local grating strength). Interferometric measurements may use a Michelson interferometer with an FBG forming one of the reflective arm and a coiled PZT cylinder with a mirrored end in the other to adjust the phase. The measurement of both the intensity reflection spectrum and the lock-in phase for each wavelength of a tunable laser diode enables the retrieval of the complex coupling coefficient using standard Fourier transform relationships. Reflectometry seems costly and generally restricted to unsaturated gratings, although algorithms have been implemented to retrieve the modulus of the coupling coefficient even for strong gratings (for which a simple Fourier transform relationship fails) [7]. Finally, the OSDR method enables the obtainment of both phase and modulus of the Bragg grating coupling strength. In this experiment, the grating is coated by a thin absorbing layer and a localized phase shift is introduced by focusing a modulated He–Ne laser beam. The transmission of the newly phase-shifted grating is then synchronously detected for any wavelength of a tunable laser diode used for testing the grating as the laser beam is scanned along the fiber.

In this paper, we describe a new, simple, and inexpensive local heating method for measuring the index modulation profile (i.e., only the modulus of the grating strength) of FBG's. A hot finger is scanned along the fiber. Therefore by heating locally some fringes, a "hot" grating comes out by which reflectivity is measured. We compare this method to the side scattering technique [4].

EXPERIMENTAL SETUP

Two separate experiments are described for the purpose of comparison. The first experiment is side scattering and the second experiment is local heating using a hot finger. For both experiments, the fiber is maintained at both extremities by two magnets on an iron support and scanned.

Side Scattering

This method is described in Krug *et al.* [4] (see Fig. 1). The beam of a helium–neon laser ($\lambda = 632.8$ nm) as a probe is focused through the side of the

¹To whom correspondence should be addressed.



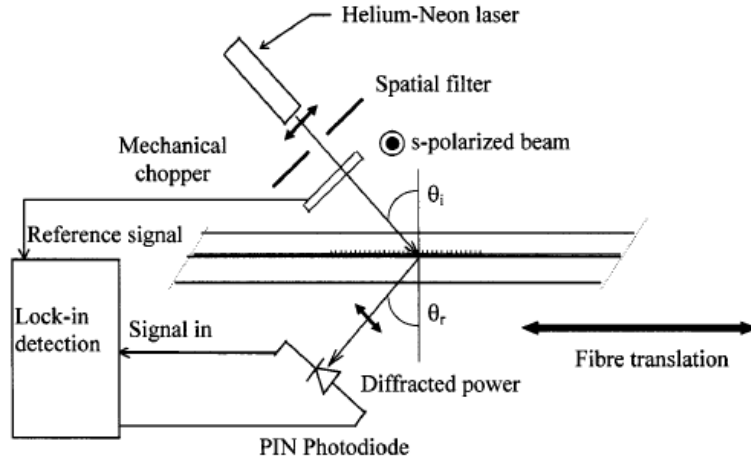


FIG. 1. Side scattering experimental setup.

fiber into its core. The first-order Bragg diffraction of the probe beam occurs at the phase-matching Bragg condition [4]

$$\sin \theta_i = n \cdot \frac{\lambda}{\lambda_B}, \quad (1)$$

where θ_i is the input angle (equal to the output angle θ_r) in air, λ is the wavelength of the probe laser, λ_B is the Bragg wavelength of the FBG, and n is the refractive index of the fiber. The diffracted beam is collected by a lens onto a PIN silicon photodiode. In our case, for a Bragg wavelength of $1.3 \mu\text{m}$, the input angle is about 45° .

As the fiber is scanned under the probe beam by moving a translation stage, the photodiode photocurrent is recorded simultaneously with the displacement. Following Krug *et al.*, we assume that the detected signal varies quadratically with the core index modulation Δn according to the scattering cross section

$$\sigma = \frac{P_{\text{diff}}(x)}{I_{\text{inc}}} \propto a^3 \cdot w^2 \cdot \Delta n(x)^2 \frac{\sin \gamma^2}{\cos \theta_1^2}, \quad (2)$$

where a is the core diameter of the fiber, w is the waist of the probe beam, and γ is the angle of polarization vector with respect to the diffraction plane.

The amount of diffracted energy strongly depends on the state of polarization of the probe beam and is maximum for *s*-polarized light (i.e., the electric vector is perpendicular to the plane, $\gamma = \pi/2$). It also depends on the impinging angle as well as the geometry of the fiber core. Therefore, calibration is needed in the event of absolute measurements. In addition, the side scattering method provides a very accurate measurement of the profile dependent on the waist dimension (typically

several micrometers), the diffracted power is easily detected by the usual photodiodes (experimental Bragg diffraction efficiencies of about 10^{-3} have been reported), and the signal-to-noise ratio can be increased further by using a synchronous lock-in detection technique (Fig. 1).

Local Heating Method

The basic principle relies on the dependence of the Bragg wavelength on temperature. In contrast to the diffraction technique, the method consists in making Bragg spectra measurements (Fig. 2). A broadband superfluorescent erbium-doped fiber source (at $1.55 \mu\text{m}$) is advantageously used because it provides a large optical power (15 dBm) and the spectrum of its amplified spontaneous emission does not exhibit ripples. The setup also comprises a three-dimensional *X-Y-Z* fiber holder with translation stages and a scanning monochromator (1200 lines/mm) of 50 pm resolution. The first translation stage sets the fiber under the hot finger (soldering iron) while the second one translates the fiber along its axis. Finally, the height of the hot finger is adjusted very closely to the fiber. For each position of the fiber, a spectrum is recorded. The number of spectra is chosen depending on the profile distribution as well as the spatial resolution (typically 40 spectra). Then, peak reflectivities are measured to retrieve spatial grating structure index modulation. Bragg spectra may be measured in transmission or in reflection. In the former mode, they are self-normalized, whereas in the latter case, an additional grating is required for normalization of reflectivity. The reflection mode is preferred because the measurement of the peak reflectivity is more accurate than in transmission mode, especially for broadband (e.g., chirped) gratings for which the baseline is somewhat difficult to estimate.

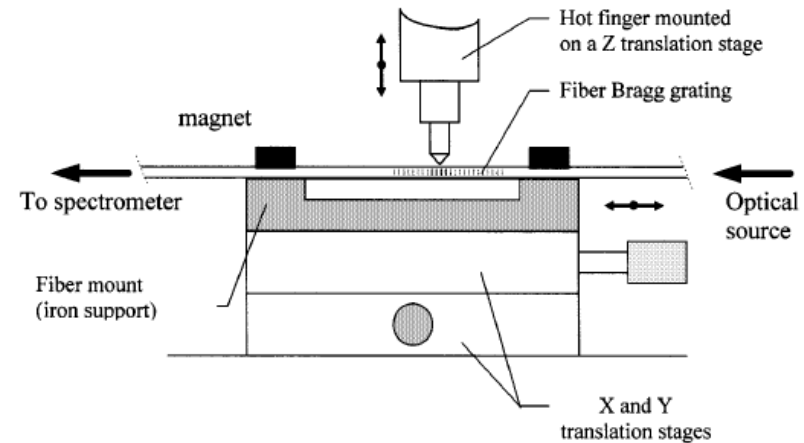


FIG. 2. Local heating experimental setup.

Since silica is a refractory material (of very low thermal conductivity), the spatial resolution is ruled by thermal convection in air that may be natural or forced. In the latter case, the spatial resolution may be rendered identical to the width of the hot finger at the expense of a lower temperature and the necessity to adjust the finger near contact.

Let us describe the behavior of the FBG spectrum under the application of a local heating. The thermal method makes use of the variation of the Bragg wavelength with temperature due to fiber expansion and the thermo-optic effect according to the usual relation [10]

$$\frac{\Delta\lambda_B}{\lambda_B} = (\alpha + \zeta) \cdot \Delta T, \quad (3a)$$

where α is the thermal expansion coefficient of silica (about $0.5 \times 10^{-6}/^\circ\text{C}$) and ζ is the thermo-optic coefficient (i.e., change of refractive index with temperature). Practically, near room temperature, the relative change of Bragg wavelength depends on temperature as follows:

$$\frac{\Delta\lambda_B}{\lambda_B} = 7.6 \times 10^{-6} \cdot \Delta T. \quad (3b)$$

The local heating manifests itself by creating another intra-Bragg grating of Bragg wavelength higher than the original one. Let λ_{BH} and R_B be respectively the Bragg wavelength and peak reflectivity of the heat part of the grating. The Bragg wavelength of the other part of the grating (“cold” grating) remains the same as that of the original grating. However, the heated fringes no longer contribute to the strength of the original grating, and as the “hot” grating strength increases, the peak reflectivity of the “cold” grating decreases accordingly because of its lesser number of fringes. Therefore, one can easily see that the spectrum of the “cold” grating cannot serve as an intensity reference in the reflection mode and thus, another extra grating λ_{Br} is used for normalization purposes. Apart from these two gratings, the temperature gradient manifests itself as a chirp in the spectral response spread between the two wavelengths λ_B and λ_{BH} . A typical spectrum is shown in Fig. 3. The precision in peak reflectivity measurement is estimated to be about 0.5% using the superfluorescent fiber source. Additional ripples stem from the fact that the “hot” grating part splits the original grating distribution into two parts that interfere in a Fabry–Perot cavity configuration. This interference pattern is stable and also gives information on the thermal diffusion length.

Let $\Delta n(x)$ and Δn_0 be the peak-to-peak modulation with respect to fiber axis x and the maximum of peak-to-peak index modulation, respectively, so that the local index is written

$$n(x) = n_{\text{mean}}(x) + \frac{\Delta n(x)}{2} \cdot \cos\left(\frac{2 \cdot \pi}{\Lambda} \cdot x\right) \quad (4)$$

and the normalized index profile is written as

$$f(x) = \frac{\Delta n(x)}{\Delta n_0}. \quad (5)$$

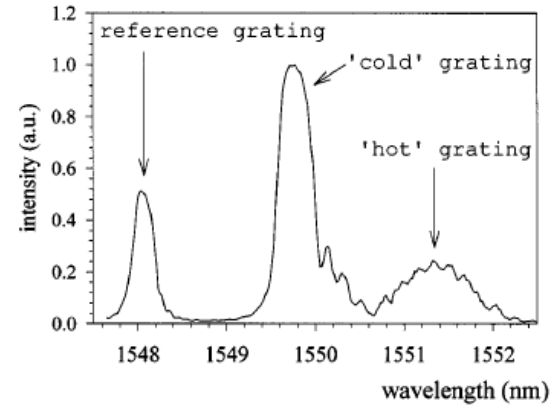


FIG. 3. Typical Bragg spectrum obtained when the hot finger is applied (grating 1 at $1.55 \mu\text{m}$, $R_c \sim 94\%$, forced convection).

The behavior of the distributed Bragg grating is described by the coupled-mode equations between forward (B) and backward (A) guided modes [11]. Both backward and forward modes are coupled by the coupling coefficient $K(x)$ as

$$K(x) = \frac{\pi}{\lambda} \cdot \eta \cdot \Delta n(x), \quad (6)$$

where η is the fraction of energy guided into the fiber core (which interacts with the index perturbation). The coupled-mode equation for the backward mode is written as

$$\frac{dA}{dx} = K(x) \cdot B \cdot e^{-2 \cdot i \cdot \Delta\beta \cdot x}, \quad (7)$$

where $\Delta\beta = \pi \cdot \left(\frac{2 \cdot n}{\lambda} - \frac{1}{\Lambda}\right)$ is a detuning parameter (difference between the propagation constant and the spatial frequency of the perturbation).

B can be taken as constant at first order for unsaturated gratings, and after integration of (7), it leads to the well-known Fourier transform relationship of the coupling coefficient

$$A(0) \approx B \cdot \int_0^\infty K(x) \cdot e^{-2 \cdot i \cdot \Delta\beta \cdot x} \cdot dx. \quad (8)$$

This relationship provides a good approximation of the reflected spectrum for weak gratings. For saturated gratings, however, this relation is no longer correct and alternative methods must be used such as transfer matrices approaches [12].

The phase-matching condition (i.e., $\Delta\beta = 0$) is obtained at the top of the Bragg grating spectrum (before application of the hot finger), according to which peak

reflectivity R_c is defined by the usual relation

$$R_c = th^2 \left(\int_0^\infty K(x) \cdot dx \right) = th^2 \left(\frac{\pi}{\lambda} \cdot \eta \cdot \Delta n_0 \cdot \int_0^\infty f(x) \cdot dx \right). \quad (9)$$

Keeping in mind that this definition is valid only for unsaturated gratings, we define the effective length of the grating as

$$L_{\text{eff}} = \int_0^\infty f(x) \cdot dx. \quad (10)$$

For a square modulation profile, the effective length reduces to the length of the profile as expected. The effective length of any grating of arbitrary index profile may therefore be simply the length of an equivalent grating of square profile of similar peak reflectivity.

Let us consider the application of a hot finger of temperature distribution $g(x)$ normalized to its maximum (i.e., $g(0) = 1$) (or, alternatively, the distribution of a probe beam intensity in the case of side scattering). The reflectivity of the “hot” grating $R_h(x)$ can be deduced by applying the relation (9) to the “hot” grating strength distribution, that is,

$$\arg th(\sqrt{R_h(x)}) = \frac{\pi}{\lambda_B} \cdot \eta \cdot \Delta n_0 \cdot \int_0^\infty f(\zeta) \cdot g(\zeta - x) \cdot d\zeta. \quad (11)$$

where ζ is a dummy variable integrated over the length of the grating.

Therefore, we obtain the following convolution relationship between the peak reflectivity of the heated and cold gratings:

$$\frac{\arg th(\sqrt{R_h(x)})}{(\pi/\lambda_B) \cdot \eta \cdot \Delta n_0} = f(x) * g(x) = L_{\text{eff}} \cdot \frac{\arg th(\sqrt{R_h(x)})}{\arg th(\sqrt{R_c})}. \quad (12)$$

In the spatial frequency domain, this equation may be also written

$$F(\nu) \cdot G(\nu) = L_{\text{eff}} \cdot \text{FT} \left[\frac{\arg th(\sqrt{R_h(x)})}{\arg th(\sqrt{R_c})} \right], \quad (13)$$

where FT means Fourier transform application. For instance, let us consider a $1/r^2$ temperature distribution $g(x)$ apart from the hot finger of 0.4 mm width (see Fig. 5).

At first glance, a simple criterion for retrieving the grating index modulation profile may be $L_{\text{eff}} \gg \int_0^\infty g(x) \cdot dx \sim 0.8$ mm (i.e., the extension of the temperature distribution is smaller than the effective length of the grating). However, Eq. (13) suggests another, finer criterion. Equation (13) shows that the spectrum of the modulation profile $F(\nu)$ is filtered by the spectrum of the temperature distribution $G(\nu)$ (i.e., the convolution equals a low-pass filtering). Consequently, high spatial

frequencies are attenuated and the measured profile is smoothed. By calculating the fast Fourier transform of the temperature distribution $g(x)$, one may verify that signals of spatial frequencies higher than about 3 mm^{-1} are attenuated by a factor of one-tenth. Let us consider an index modulation ripple of 10% amplitude (relative to the maximum) and of spatial period 0.3 mm; the measured amplitude is than 1%, which is about the accuracy. Consequently, we can anticipate that the shortest spatial period than can be observed with the local heating method is of the order of 300 μm with such a temperature distribution.

The smaller the number of fringes selected by the hot finger, the better the spatial resolution is and the strength of the “hot” grating becomes small enough so that Eq. (12) reduces to

$$\frac{2\sqrt{R_h(x)}}{(\pi/\lambda_B) \cdot \eta \cdot \Delta n_0} = f(x) * g(x). \quad (14)$$

Consequently, the amount of longitudinal and side-scattered energies both vary like the square of the local index modulation. The signal-to-noise ratio requires a minimal number of fringes imposed by the detection of the hot grating reflectivity. It should not be overlooked that Eq. (14) provides an easy self-normalized measurement (actually, this is not the case in the side scattering method, which critically depends on focusing conditions).

EXPERIMENTAL

Gratings of arbitrary index profiles have been photo-written using a modified Lloyd mirror configuration [13]. This setup has been modified in such a way that it incorporates a reception mirror similar to the folding mirror, placed symmetrically to it with respect to the center of the grating. This mirror sends the emerging UV light toward a UV CCD camera in a constant direction whatever the angle of the fiber support is. This modified setup has a decided advantage over the previous classical Lloyd set-up in that it enables the accurate control of the energy distribution of both folded beams to provide any arbitrary distribution of average refractive index (mean index) and index modulation profile. For the purpose of demonstration, three gratings have been photo-written along with the recording of their UV interfering beam profiles. Grating 1 is apodised, and has a peak-to-peak index modulation of 3.8×10^{-4} and a peak reflectivity of 94% (see Fig. 3). Grating 2 has a square index profile, and grating 3 shows index modulations. Then, those gratings were scanned using the two methods previously described (i.e., by local heating and side scattering methods).

RESULTS AND DISCUSSION

Figure 3 shows the Bragg spectra under the application of the hot finger. The Bragg spectrum of the “hot” grating is shifted by an amount of wavelength shift dependent on the fiber temperature (typically 100 to 150°C). Let us consider a maximum local temperature of 150°C (limited by the destruction of the coating

polymer); the corresponding spectral shift is about 1.8 nm (at 1.55 μm). Therefore, highly chirped gratings (> 2 nm spectral width) cannot be easily studied using the method of local heating.

Figure 4 shows the modulation profile of the three gratings tested as obtained by the local heating and side scattering methods. The local index modulation mea-

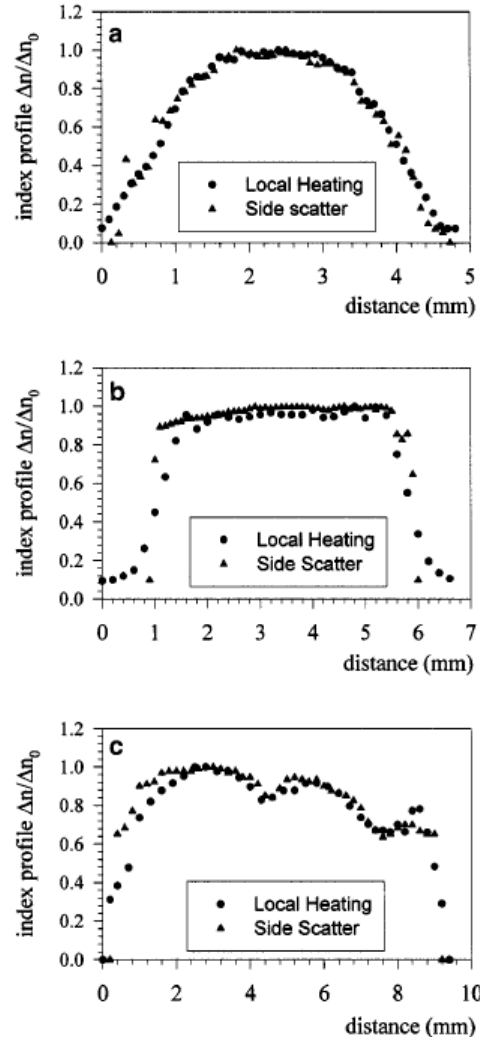


FIG. 4. Index modulation profiles of (a) grating 1 (apodised, $L = 3.15$ mm); (b) grating 2, $L = 4.78$ mm and; (c) 3, $L = 7.5$ mm, as obtained with the local heating and side scattering methods.

sured with the side scattering method is calculated using (2), whereas it is calculated using (12) in the local heating measurement. The effective lengths of the three gratings are listed in Table 1. A very good agreement is found between these two methods. As expected, the side scattering method displays a better accuracy than the local heating method does, as revealed by the observation of the edge of the modulation profile of grating 2. Moreover, gratings 1 and 3 show some irregularities not observed with the local heating method. These irregularities are expected to arise from dust or diffraction imperfections in folded UV beams on the fiber. Grating 3 shows the ability to detect local index variations.

A method for retrieving the modulation profile is to take the Fourier transform of (12), dividing by the Fourier transform of the hot finger temperature distribution, and finally taking the inverse Fourier transform. Attempts to deconvolute the measured profile lead to great difficulties because the inversion in the FFT domain is greatly corrupted by noise, and moreover, this method is advantageous only when the Fourier transform of the $g(x)$ function is very accurately known, which is not the case practically. Conversely, the comparison of experimental and theoretical "hot" grating reflectivities is made by convoluting the theoretical profile with the temperature distribution of Fig. 5. With this aim in view, the modulation profile of grating 2 obtained by the local heating method is compared to the convolution of the profile as obtained by the side scattering method with the temperature distribution of the hot finger (Fig. 5) (granted that the precision in side scattering experiments are about one order of magnitude higher than in local heating). The profile obtained is of course considerably smoothed out and matches well the experimental one, which in turn validates the temperature distribution. Since the index profile of grating 2 is a square profile, the extreme parts of the profile measured by local heating indicate the decay behavior of the temperature distribution and the width of the hot finger broadens the index profile. The temperature distribution is then adjusted to fit the experimental local heating measured profile (plateau of 0.4 mm width with two $1/r^2$ decays).

CONCLUSION

We describe a new method of localizing a Bragg grating along the fiber length and retrieving its index modulation profile using a hot finger scanned along the fiber. Results obtained from this local heating method have been compared to

TABLE 1
Effective Lengths of the Three Gratings Tested as Measured by (a) Local Heating and (b) Side Scattering Methods

| | Grating number | | | | | |
|--------------------------------------|----------------|------|------|------|------|------|
| | 1 | | 2 | | 3 | |
| Method: | LH | SS | LH | SS | LH | SS |
| Effective length (mm) \pm 0.02 mm: | 3.22 | 3.15 | 4.75 | 4.78 | 7.51 | 7.50 |

Note. LH, local heating; SS, side scattering.

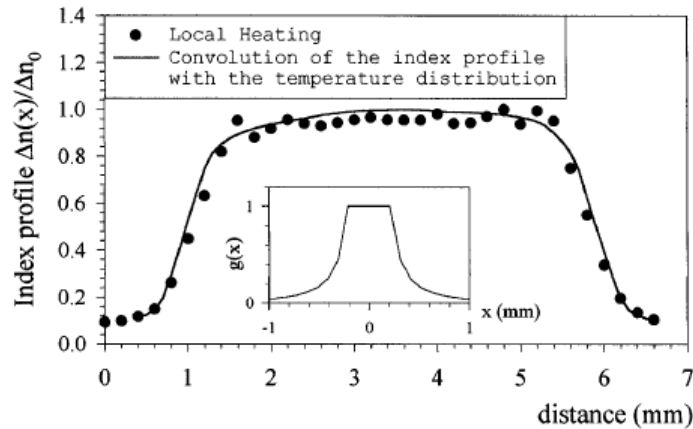


FIG. 5. Comparison of experimental and theoretical index profiles of grating 2 as obtained using the local heating method. Inset shows the temperature distribution used for the convolution procedure.

those obtained from the side scattering method [4]. If only the localization of the grating matters, we prefer the local heating method over side scattering because the easy positioning of the fiber allows a quick localization to be done. Otherwise, these two methods do not convey the same advantages in retrieving the index modulation profile although they are both inexpensive and easy to use. These two methods both have inherent advantages and drawbacks listed in Table 2. The side scattering method provides a higher spatial resolution and is rapid but requires stripping of the coating off the fiber and careful preparation of the surface of the fiber (which procedure is also time consuming). Conversely, any arbitrarily conditioned grating might be studied using the local heating method (e.g., recoated gratings), which provides an absolute measurement (i.e., the peak reflectivity) whatever the temperature is (granted that it is high enough to distinguish both “cold” and “hot” peaks) and the measurement is self-referenced (the greater inaccuracy stems from the value of the modal fraction of energy, which usually ranges from 0.7 to 0.8). Moreover, no accurate positioning is required in the local heating method, whereas in the side scattering experiment the probe beam must be accurately focused into the fiber core to optimize diffraction efficiency, and the fiber has to be carefully aligned with respect to the probe beam in order to keep the diffraction efficiency constant as the fiber is scanned. There are no similar limitations for the local heating method, which is particularly interesting for small-core fibers (e.g., fibers used for nonlinear single-mode fiber optics). Many other applications in sensors and instrumentation may advantageously use the local heating method complementarily to the side scattering method. However, there exist inherent limitations in the local heating method which are, first, a lesser spatial resolution and, second, the inability to measure highly chirped gratings (say

TABLE 2
Comparison of Characteristics of the Local Heating and Side Scattering Methods for the Measurement of the Index Modulation Profiles of FBGs

| Characteristics | Methods | |
|--|--|---|
| | Local heating | Side scattering |
| Amplitude of the modulation index Δn_0 | May be considered as a reference method for determining the value of the index modulation (it requires only estimation of the fraction of modal power η) | Requires a calibration (depends on focusing conditions) |
| Relative precision in modulation index | About 1% | Better than 1% |
| Sample preparation | none | Fiber stripped off and clean surface |
| Grating types | Method not suited for highly chirped gratings (> 2 nm) as dispersion compensators and very short gratings (length < 1 mm) | Every type of grating |
| Spatial resolution | Depends on heating method (laser or soldering iron) and on convection in air (typ. $300 \mu\text{m}$) | Depends on the waist of the probe beam (typ. $10 \mu\text{m}$) |
| Simplicity | Easy positioning | Delicate positioning mostly for small core fibers; requires a perfect alignment (constant diffraction efficiency) |

of spectral width larger than 2 nm), and this method could not be used—as is—for studying actual dispersion compensators, for instance.

Laser impacts may be substituted for by soldering irons or hot wires to operate under temporary heating regime to achieve localized heating even on substrates of higher thermal conductivity than silica. Both methods lend themselves to real-time monitoring using motorized translation stages.

Finally, the time to perform a set of local heating measurements is still long (10 to 20 min) but may be reduced by using a tunable laser diode operating in scanning mode.

REFERENCES

- [1] M. G. Xu, A. T. Alavie, R. Maaskant, and M. M. Ohn, “Tunable fibre bandpass filter based on a linearly chirped fibre Bragg grating for wavelength demultiplexing,” *Electron. Lett.*, vol. 32, 1918 (1996).
- [2] S. Gupta, T. Mizunami, and T. Shimomura, “Computer control of fiber Bragg grating spectral characteristics using a thermal head,” *J. Lightwave Technol.*, vol. 15, 1925 (1997).

- [3] G. R. Fox, C. A. P. Muller, N. Setter, D. M. Costantini, N. H. Ky, and H. G. Limberger, "Wavelength tunable fiber Bragg grating devices based on sputter deposited resistive and piezoelectric coatings," *J. Vac. Sci. Technol. A*, vol. 15, 1791 (1997).
- [4] P. A. Krug, R. Stolte, and R. Ulrich, "Measurement of index modulation along an optical fiber Bragg grating," *Opt. Lett.*, vol. 20, 1767 (1995).
- [5] M. Froggatt, "Distributed measurement of the complex modulation of a photo-induced Bragg grating in an optical fiber," *Appl. Opt.*, vol. 35, 5162 (1996).
- [6] M. M. Ohn, S. Y. Huang, R. M. Measures, and J. Chwang, "Arbitrary strain profile measurement within fibre gratings using interferometric Fourier transform technique," *Electron. Lett.*, vol. 33, 1242 (1997).
- [7] E. Brinkmeyer, "Simple algorithm for reconstructing fibre gratings from reflectometric data," *Opt. Lett.*, vol. 20, 810 (1995).
- [8] P. Lambelet, P. Y. Fongjallaz, H. G. Limberger, R. P. Salathé, Ch. Zimmer, and H. H. Gilgen, "Bragg grating characterization by optical low-coherence reflectometry," *IEEE Photon Technol. Lett.*, vol. 5, 565 (1993).
- [9] E. Brinkmeyer, G. Stolze, and D. Johlen, "Optical space domain reflectometry (OSDR) for determination of strength and chirp distribution along optical fiber gratings," in *Optical Fiber Sensors Conference*, Williamsburg, USA, Optical Society of America, 1997.
- [10] G. Meltz and W. W. Morey, "Bragg gratings formation and germanosilicate photosensitivity," in *International Workshop of Photo-induced Self-Organization Effects in Optical Fiber*, (F. Ouellette, Ed.), Proc. SPIE 1516, pp. 185–199.
- [11] A. Yariv, *Quantum Electronics*, 3rd Ed., p. 661, Wiley, New York.
- [12] M. Yamada and K. Sakuda, Analysis of almost-periodic distributed feedback slab waveguides via a fundamental matrix approach, *Appl. Opt.*, vol. 26, 3474 (1987).
- [13] C. Martinez and P. Ferdinand, Phase-shifted fibre Bragg grating photo-writing using a UV-phase plate in a modified Lloyd mirror configuration, *Electron. Lett.*, vol. 34, 1687 (1998).



NICOLAS ROUSSEL was born in Fontenay-sous-Bois in July, 1972. He received a diploma of technician in optoelectronics in 1993 (*Lycée Fresnel, Paris 15*). He is currently continuing his education at *Conservatoire National des Arts et Métiers (Paris 3)* to receive a diploma of engineer in optical metrology and instrumentation. In 1997, he worked at LETI (CEA—Technologies Avancées) (Saclay, France) on fiber Bragg grating photo-inscription and reliability. In 1998, he worked at *Institut National de Métrologie* where he was involved in the testing of rubidium cells used for wavelength standardization.



SYLVAIN MAGNE was born in Nanterre, France on November 22, 1965. He received a diploma of technician from *Institut Universitaire de Technologie—Mesures Physiques* (Grenoble, France) in 1986. He received a diploma of engineer in physics from the *Institut National Polytechnique de Grenoble* in 1989 and a *Diplôme d'Etudes approfondies* in instrumentation from *Université Joseph Fourier* (Grenoble, France) in 1989. He received a *Diplôme de Doctorat* from the Université of Saint-Etienne, France in 1993. From 1990 to 1993, he worked at LETI (CEA—Technologies Avancées) (Saclay, France) jointly with *Laboratoire de Traitement du Signal et d'Instrumentation* (CNRS—Saint-Etienne, France) on rare-earth-doped fiber lasers and spectroscopy. His current researches include fiber Bragg grating sensors and networks for advanced structure monitoring, optically stimulated luminescence dosimetry, and Raman spectroscopy. He is the author of 14 publications and holds five patents. Dr. Magne is a member of the *Société Française d'Optique*.



CHRISTOPHE MARTINEZ was born in Pertuis, France, on March 10, 1972. He received a diploma of engineer from the *Ecole Supérieure d'Optique* (Orsay, France) and a *Diplôme d'Etudes Approfondies* in optics and photonics in 1995 from the University of Orsay (France). Since then, he has been working on a Ph.D. thesis concerning fiber Bragg grating photoinscription and related devices. M. Martinez is the author of four publications and one patent on fiber Bragg grating photo-inscription techniques. M. Martinez is a member of the *Société Française d'Optique*.



PIERRE FERDINAND was born in Paris, France on June 27, 1955. He received an M.S. in physics in 1978 from the *Université Pierre et Marie Curie* (Paris VI), France and a *Diplôme d'Etudes Approfondies* in plasma physics in 1980, from the University of Paris XI, Orsay, France. In 1982, he received a *Doctorat de troisième cycle* in physics, from the University of Paris XI, and in 1990 he received a *Doctorat d'Etat es Sciences*, from the University of Nice, France. From 1980 to 1992, he worked in the R & D Division of *Electricité de France*, on many optical sensing topics such as stabilized optical sources (transverse Zeeman Laser), optical sensors, and optical fiber sensors (optical fiber ammeter, OTDR-POTDR, OFDR, FMCW, coherence multiplexing). In 1992, he joined LETI (CEA—Technologies Avancées), Saclay, France, and has engaged as head of the Optical Measurement Laboratory. His current researches include optical components, fiber Bragg grating technology, optical fiber sensors and networks for advanced structure monitoring, radiation, and gas detection. Dr. Ferdinand holds eight patents, is author of one book and about 40 research publications on optical fiber sensors and related subjects. He is a fellow of the *Société Française d'Optique*, of the European Society, and of the *Société des Electriciens et des Electroniciens de France*. Dr. Ferdinand is also a fellow of the Optical Society of America and member of the technical committee of the International Optical Fiber Sensor Conference.